OPTICAL PROPERTIES OF $GdAlO_3:Cr^{3+}$

M.A. Aegerter, Prof. Dr. and H.C. Basso

Instituto de Física e Química de São Carlos, Universidade de São Paulo
13560 São Carlos (SP) Brazil

and

H.J. Scheel

IBM Zurich Research Laboratory
8803 Rüschlikon, Switzerland

Abstract

Single crystals of $GdAlO_3$, inclusion-free and homogeneously doped with Cr^{3+}, have been flux-grown using a slow-cooling technique. The optical properties - absorption, excitation and luminescence spectra, polarization behavior and decay time of emissions - have been measured for isolated Cr^{3+} ions as well as first-nearest-neighbor parts of Cr^{3+} in the paramagnetic and antiferromagnetic phase (Néel temperature T_N=3.9 K).

I Introduction

The uniaxial antiferromagnet compound $GdAlO_3$ belongs to space group D_{24}^{16}-Pbnm with four distorted perovskite units in the true orthorhombic cell having lattice constants a=5.345 Å, b=5.616 Å and c=7.668 Å.[1,2] Magnetic phase diagrams showing the paramagnetic ↔ spin-flop ↔ satured paramagnetic transitions have been determined as a function of temperature and magnetic field.[3,4] The antiferromagnetic phase transition occurs at a Néel temperature T_N=3.89 K. Recent measurements have now ascertained unambiguously that the Gd^{3+} spin structure aligns along the a axis[5,6] rather than the b axis as claimed earlier.[3]

Up to now, few optical studies have been made on this material although they offered clear advantages over the magnetic techniques as they provide information on the ground and excited states of ions. As the lowest energy transitions of Gd^{3+} measured in absorption fall in the UV region and as the ground state of this ion is complex ($^8S_{7/2}$), all the studies which tended to analyze the effects of the magnetic phase transitions on the physical properties of ions have been done on samples doped either with trivalent rare-earth impurities or with ions of the iron transition group[7-15] which substitutes for Gd^{3+} or Al^{3+} ions, respectively. Due to the difficulty of growing good crystals of $GdAlO_3$, all the results have so far been observed either with powder or crystals having poor optical quality.

Most of the optical studies using transition ions of the iron group as dopant have been done with Cr^{3+}. Blazey and Burns[11] measured the $^2E \rightarrow {}^4A_2$ flourescence of isolated Cr^{3+}, and interpreted the luminescence spectrum consisting of a broad emission around 730 nm with four resolved peaks by including a Heisenberg-type magnetic interaction of the Cr^{3+} with the neighboring Gd^{3+} (J=2,3 cm^{-1}) and magnetic interaction between Gd^{3+} themselves. Murphy and Ohlmann[12] and Ohlmann et. al.[13] reported an extensive study of the absorption and fluorescence spectra of isolated Cr^{3+}, and describe the forbidden $^4A_2 \leftrightarrow {}^2E$ transitions in terms of an isotropic exchange interaction $JS_{Cr} \cdot \Sigma S_{Gd}$ with J=2,1cm^{-1} for the S=3/2 ground state and J'=3,2cm^{-1} for the S=1/2 excited state. The decrease of the splitting between the fluorescence peaks observed below 3.9 K have been related to the onset of the antiferromagnetic ordering. More recently, we studied the effect of an external magnetic field on the fluorescence spectra at liquid-helium temperature.[10] The resulting splitting was explained in terms of a modified molecular-field approximation which incorporated the effect of the spin fluctuation;[11] an exchange constant of 1.2 cm^{-1} was found for the relaxed excited state which is quite different from that calculated from the absorption data.

One of us (H.J.S.) has succeeded in growing large single crystals of $GdAlO_3$, inclusion- and crack-free and homogeneously Cr^{3+}-doped. In view of the disparate conclusions obtained till now and as $GdAlO_3$ is still potentially an outstanding candidate for high power-pulsed lasers, we have started a complete spectroscopy study of optical quality $GdAlO_3:Cr^{3+}$. We report here our first detailed measurements of absorption, excitation, luminescence and decay time of isolated and pairs of Cr^{3+}. The experimental procedure as well as results are given in Sec. II, and a discussion and tentative explanation in Sec. III.

II Experimental

A. Crystal Preparation

Large undoped $GdAlO_3$ crystals have been grown from PbO-PbF_2-B_2O_3 solutions.[16,17] However, growth of Cr-doped crystals is more difficult because: i) the platinum crucibles are much more corroded at the high growth temperatures, probably due to the oxidation of Cr^{3+} to Cr^{6+} [$Cr_2O_3 + 1.5\ O_2 \rightleftarrows 2CrO_3$ (-5.3 Kcal) at $T < 1000\ ^{\circ}C$] and the resulting reduction of PbO to Pb which then alloys with the platinum; ii) the Cr^{3+} concentration during the slow-cooling crystal-growth process is decreasing due to the above equilibrium and by incorporation in the crystals ($k_{eff} > 1$), resulting in crystals of high Cr concentration in the center and practically no Cr at the periphery of the crystals. In order to reduce this effect, Remeika[18] proposed using Bi_2O_3-based solvents which, however, have the disadvantage that a few percent Bi^{3+} are incorporated in the rare-earth compound crystals due to the crystal-chemical similarity (valency, ionic radii) or Bi and the rare-earth ions.

We used lead-based fluxes, added PbO_2 to minimize the reduction of PbO, and reduced the cooling interval by stopping the experiment around 1000 °C instead of 900 °C. The chemicals of analytical grade (82.5 g Gd_2O_3, 22.5 g Al_2O_3, 0.75 g Cr_2O_3, 240 g PbO, 225 g PbF_2, 15 g B_2O_3, 3 g PbO_2) were mixed and premelted in a 180 cm^3 platinum crucible which was then sealed by argon-arc welding leaving a tiny hole to prevent overpressure. After soaking for 15 hours at 1300 °C, the temperature was oscillated between 1230 and 1270 °C to reduce the number of nuclei.[19] Starting from 1270 °C, a cooling rate of $0.3\ ^{\circ}h^{-1}$ was applied until about 1000 °C when the rest melt was decanted through holes punched into the lid. After cutting off the lid, the residual flux was dissolved in hot diluted nitric acid, and the crystals up to 1 cm in size, with inclusion and crack-free regions up to 5 × 5 × 5 mm, were removed from the bottom and walls of the crucible. To grow larger crystals, the accelerated crucible-rotation technique has to be applied.[16,17] Two crystals were available. The first one, called hereafter "crystal I", had a low, uniform Cr^{3+} concentration (~0.1%) and a perfect crystallographic structure. It was used to study the optical properties of isolated Cr^{3+} ions. The second one, called hereafter "crystal II", was a twinned crystal and had an unhomogeneous Cr^{3+} concentration (~1%). This crystal was mainly used to get preliminary data of the optical properties of pairs of Cr^{3+}.

The crystallographic structure and the orientation were redetermined for crystal I using an automatic difractometer Enraf-Nonius CAD-4. The former results were fully confirmed.[1,2]

B. Optical Measurements

All the measurements were done using a Janis Super Varitemp cryostat whose temperature was regulated by a Lake Shore DTC-500 temperature controller ($T > 4K$) and a Lake Shore vacuum regulator valve 329 ($1.5\ K < T < 4K$). Most of the absorption measurements were done in a Cary 17 spectrophotometer. However, for higher resolution we also built a double-beam dual-frequency chopped spectrophotometer using as a source a 150 W Xe lamp (Oriel 7340) focused on a 50 cm Jarrel-Ash (82020) monochromator.

Most of the excitation spectra were recorded using the same excitation source, the detection being done either with one or two 25 cm Bausch and Lomb monochromators connected in series, followed by an EMI 9555 or 9559 QB photomultiplier, PARR lock-in (124 A or 5204) and recorder WW 312. For the luminescence measurements, both monochromators were exchanged.

However, these techniques did not allow analysis of the $^4A_2 \leftrightarrow {}^2E$ excitation and luminescence spectra originating from excitation in these bands as both spectra are almost superimposed. For that, we devised a special technique[20] using a two-window chopper (PARR 192) and a wheel having an odd number of apertures. It was placed in the set-up in such a manner that the luminescence was only detected during its decay after the period of excitation (Fig. 1). In such a way, the stray light occurring during excitation was completely eliminated, and superimposed excitation and luminescence spectra and even decay time could be analyzed without any further problems to a resolution of 1.5 Å.

The measurements of the decay time were performed using a dye laser (Spectra Physics 375) pumped by a cw argon laser (Spectra Physics 166). This source was chopped with a mechanical obturator (Ealing 22-8411) followed by a slit-chopper (PARR 125-A); the pulses were $\Delta t = 200\ \mu s$ wide and had a variable separation of 30 to 120 ms. The time variation of the luminescence was measured with an EMI 9659 QB photomultiplier and averaged on a PARR 4203 Signal averager. The results of around 500 pulses were then sent on a recorder (HP 7004 B) and analyzed by hand. Some measurements of time-resolved luminescence were also taken to separate the contribution of isolated Cr^{3+} from that of the Cr^{3+} pairs. For this purpose, a boxcar integrator (PARR 160) was used in place of the signal averager.

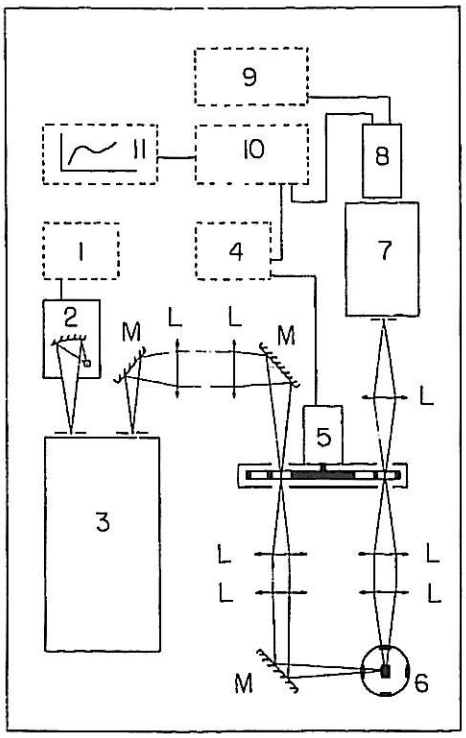

Fig. 1. Experimental set-up for measuring excitation spectra with high resolution: 1) power supply for Xe lamp (Oriel 6123); 2) Xe lamp 150 Wf/8 (Oriel 7340); 3) Jarrel-Ash 50 cm monochromator (82020); 4) power supply for chopper (PARR 192); 5) chopper (PARR 192-93); 6) liquid-helium cryostat (Janis Supervaritemp); 7) Bausch & Lomb monochromator (33-86-79); 8) photomultiplier (EMI 9559 QB, Ext S20); 9) power supply for photomultiplier (Keithley 224); 10) lock-in (PARR 5204) or boxcar (PARR 160); 11) recorder (W+W312); L) convergent lens (Oriel); M) Al mirror (Oriel).

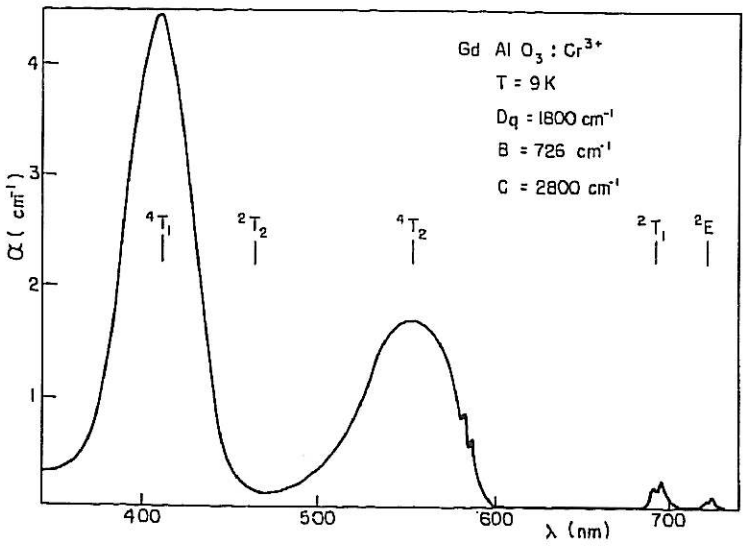

Fig. 2. Absorption spectrum of $GdAlO_3:Cr^{3+}$ at 9 K. A broad structureless UV tail has been subtracted. The position of the bands $^4T_1$, $^2T_2$, $^4T_2$, $^2T_1$ and ^2E has been calculated with the parameters shown in the figure.

C. Single-Ion Properties

a) Above the Néel Temperature (T > 3.9 K): The general structure of the single Cr^{3+} ion absorption spectrum in $GdAlO_3$ appears similar to that of Cr^{3+} ions in ruby, typical of that found for this impurity when surrounded by six oxygen ions in an almost octrahedral symmetry. Figure 2 shows such a spectrum measured at 9 K with crystal I.

Four groups of lines or bands can be easily identified as belonging to the following transitions: $^4A_2 \rightarrow {}^2E$, $^4A_2 \rightarrow {}^2T_1$, $^4A_2 \rightarrow {}^4T_2$ and $^4A_2 \rightarrow {}^4T_1$. The weak $^4A_2 \rightarrow {}^2T_2$ transitions could not be found. All these transitions lie on a long UV tail whose origin has not yet been analyzed but which also appears in undoped samples. It is probably due to the f-d transitions of Gd ions. Owing to the relatively large width of all the absorption lines, their positions have only been computed in the cubic-field approximation as a function of the Raccah parameter by using Tanabe's and Sugano's energy matrices.[21] The best fit gave the following values: Dq=1800 cm^{-1}, B=726 cm^{-1} and C=2800 cm^{-1}. These values give a definitely better fit than the values given earlier.[7,13] The positions of the calculated bands are also shown in the figure.

Excitation in any one of the bands gives rise to a complicated luminescence spectrum slightly Stokes-shifted with regard to the $^4A_2 \rightarrow {}^2E$ absorption transition. It appears as three (probably four) broad lines partially superimposed and whose separation at LHeT is of the order of 20 cm^{-1}. Figure 3 shows our results taken at 9 K. On the left side of the figure, we have represented the unpolarized absorption spectrum of the two lowest transitions $^4A_2 \rightarrow {}^2E$, $^4A_2 \rightarrow {}^2T_2$, and on the right side, the $^2E \rightarrow {}^4A_2$ luminescence spectrum. They are identical to those previously observed by others.[11-13]

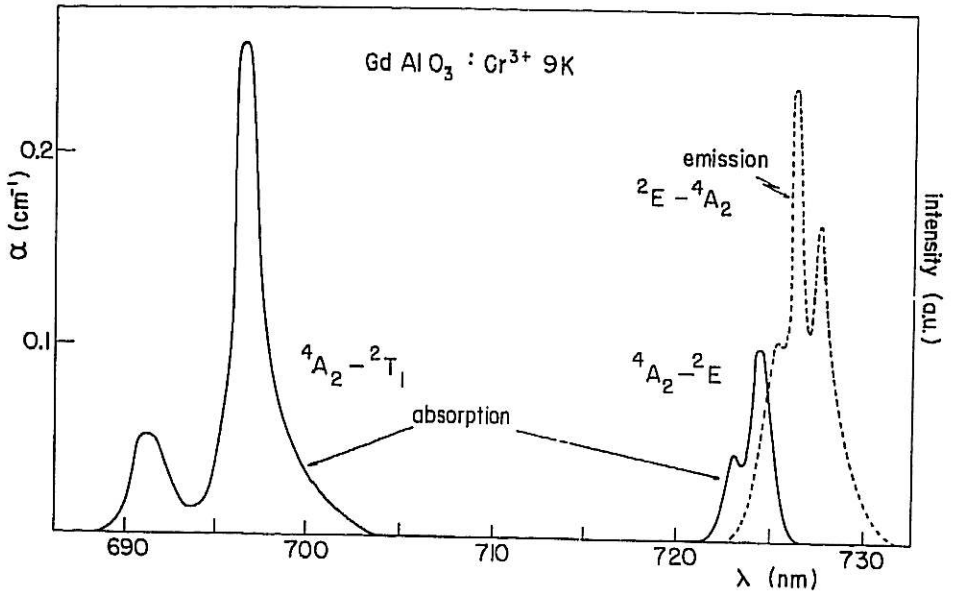

Fig. 3. On the left side: $^4A_2 - {}^2T_1$ and $^4A_2 - {}^2E$ absorption spectra. On the right side: $^2E - {}^4A_2$ emission spectrum. T=9 K.

Theoretical models have already been proposed to explain the positions and the shape of the bands. For instance, Murphy and Ohlmann[12] treated isolated Cr^{3+} ions in a pure cubic-field approximation with an isotropic ferromagnetic exchange interaction with the eight surrounding Gd^{3+} ions of the form $H' = -J\vec{S}_c \Sigma \vec{S}_i$, where $\vec{S}_c$ is the spin of the Cr^{3+} (3/2 in the ground state and 1/2 in the excited state) and $\vec{S}_i$ is the spin of Gd^{3+} (7/2). This model explains relatively well the positions and the shape of the $^4A_2 \rightarrow {}^2E$ absorption bands (J=3.2 cm^{-1}) and $^2E \rightarrow {}^4A_2$ emission bands (J=2.1 cm^{-1}). The $^4A_2$ level appears fourfold split while the ^2E level is twofold split. The transitions observed at low temperature are the following:

Absorption	λ = 722.3 nm	$\lvert S + 3/2 \rvert$	$\rightarrow$	$\lvert S - 1/2 \rvert$
Absorption	λ = 723.6 nm	$\lvert S + 3/2 \rvert$	$\rightarrow$	$\lvert S + 1/2 \rvert$
Emission	λ = 725.8 nm	$\lvert S + 1/2 \rvert$	$\rightarrow$	$\lvert S - 3/2 \rvert$
Emission	λ = 726.5 nm	$\lvert S + 1/2 \rvert$	$\rightarrow$	$\lvert S - 1/2 \rvert$
Emission	λ = 727.3 nm	$\lvert S + 1/2 \rvert$	$\rightarrow$	$\lvert S + 1/2 \rvert$
Emission	λ = 728.0 nm	$\lvert S + 1/2 \rvert$	$\rightarrow$	$\lvert S + 3/2 \rvert$

where $S = \sum_i s_i$, $0 \leq S \leq 28$.

Let us note that also within a mean-field approximation, Helman[15] later included the Gd^{3+}-Gd^{3+} interaction to explain the temperature variation of the luminescence peaks. However, several inconsistencies can already be noted:

i) The absorption spectrum is better resolved than the emission spectrum although the widths of the bands have similar values because the separation between the peaks in absorption (~30 cm^{-1}) is larger than in emission (~20 cm^{-1}) which is in contradiction to the model.

ii) The two $^4A_2 \rightarrow {}^2E$ absorption lines shift towards lower energy while keeping their separation constant contrary to the emission bands which practically do not shift their positions, except the high energy line which shifts towards higher energy when the temperature increases.

iii) The polarization behavior of the lines (see below) is totally inconsistent with the models.

Let us now present some new results: Figure 4 shows the absorption spectrum of the $^4A_2 \rightarrow {}^2E$ transitions measured under polarized light propagating along the c axis with E vector along the a or b axis. The same behavior was measured in the excitation spectrum. The two broad lines appear partially polarized and two new bands (which were barely visible

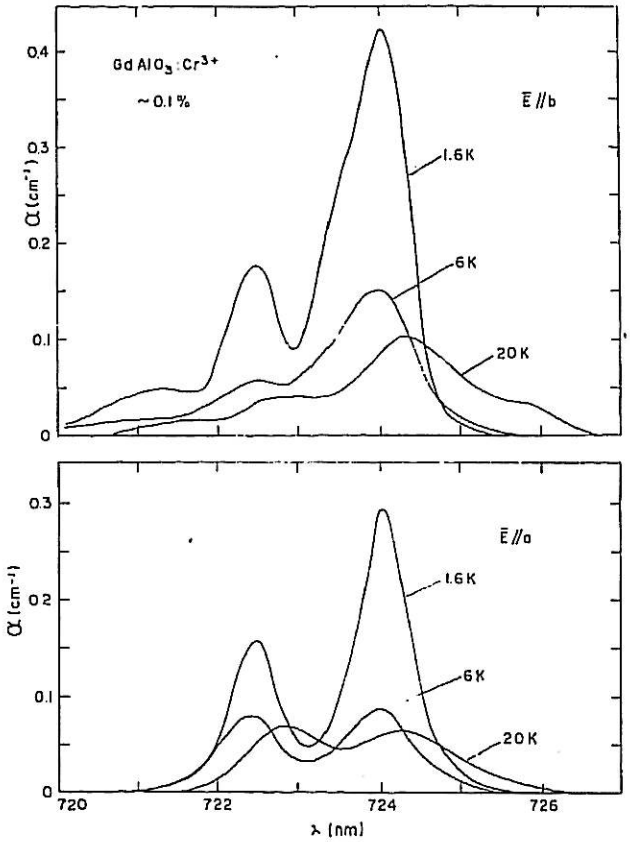

Fig. 4. Polarized absorption spectra of the $^4A_2 \rightarrow {}^2E$ transition; light propagates along the c axis with $\vec{E}$ vector along the a and b axes, respectively.

in the unpolarized spectra), appear completely polarized along the b axis, one on the high energy side around 721.5 nm and the other on the high energy side of the lowest energy line around 723.5 nm. These polarization states can be observed even at higher temperatures (up to 60 K!) but the ratio of the intensities in each configuration changes. For example, for the E vector parallel to the a axis, $I_{724}/I_{722.5}$ decreases with increasing temperature and becomes smaller than one. Moreover, the transition observed around 726 nm at temperature higher than 20 K and which probably originates from the thermally populated $|S+1/2|$ ground-state level: $^4A_2\,|S+1/2| \rightarrow {}^2E\,|S+1/2|$ appears totally polarized parallel to the b axis.

The transition $^4A_2 \rightarrow {}^2T_1$ (Fig. 3) consists of two peaks located at 691.5 nm and 697.0 nm completely polarized along the b axis, whatever the temperature. These effects were measured either in absorption or in the excitation spectrum. The broad transition $^4A_2 \rightarrow {}^2T_1$ also appears slightly polarized (of the order of 10%) along the b axis. These results cannot be explained with the previous theories.

b) Below the Néel Temperature ($T < 3.9$ K): The absorption spectrum of the $^4A_2 \rightarrow {}^2E$ transitions at the lowest temperature reached in the antiferromagnetic phase is shown in Fig. 4. The new extra lines, completely polarized along the b axis are now easily seen. As the temperature decreases, the bands slightly shift towards lower energy and their intensity increases drastically. A similar behavior has been observed in the luminescence spectra (Fig. 5). As the temperature is lowered, the emission intensity increases and the width of the bands diminishes. The middle peak does not change its position, but the higher and lower energy ones move towards it. No definite polarization has been observed. The most interesting result is shown in Fig. 6 which summarizes the results of the emission transition probability. Above T_N, the decay time is purely exponential and remains practically constant (τ=15 ms) as a function of temperature (decrease of 20% between 4.2 K and 300 K). Below T_N, it remains exponential but gradually diminishes with the temperature. The curve adjusted to the experimental results is given by:

$W - W_O$ = $a\sigma^2(T)$ with $\sigma(T) = M(T)/M(T=0) = B_S(T,\sigma(T))$
$W = \tau^{-1}$ transition probability
$W_O = \tau_O^{-1}$ transition probability measured just above T_N; $W_O = 66.7\ s^{-1}$
$\sigma(T)$ relative magnetization of the Gd ions sublattice $M(T)/M(T=0)$
$B_S(T,s(T))$ Brillouin function
a proportionality factor $a = 66.3\ s^{-1}$.

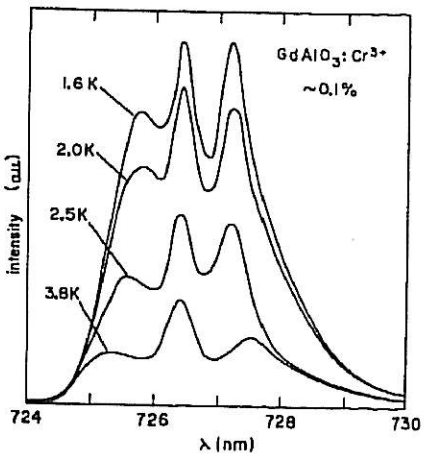

Fig. 5. Emission spectra measured in the antiferromagnetic phase.

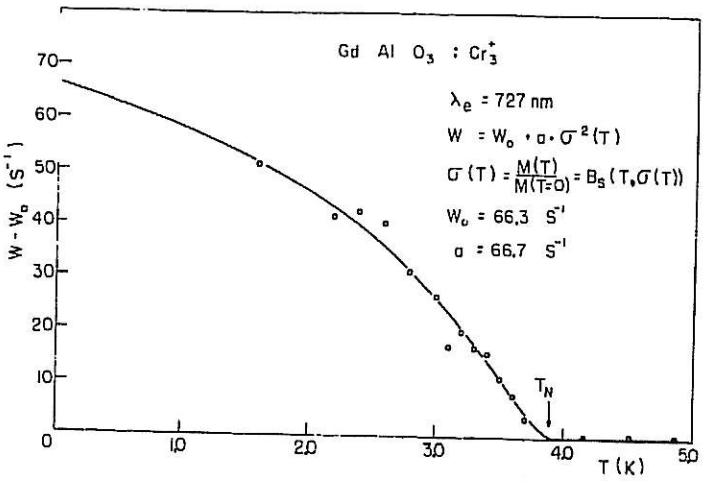

Fig. 6. Variation with temperature of the transition probability $W(T) - W_O$ of the emission of isolated Cr^{3+} in $GdAlO_3$ (λ=727 nm). The curve has been computer adjusted (see text).

D. Cr^{3+}-Pair Properties

Crystal II has a higher concentration of Cr^{3+} but is not homogeneously doped. Most of the properties described previously have also been observed with this crystal. However, no polarization effects have been measured; this indicates that the sample is probably a twinned crystal. Moreover, the decay curve of isolated Cr^{3+} is no longer a pure exponential. The signal intially decreases rapidly and eventually approaches, after a delay of ~10 ms, an exponential decay having the same time-constant value as found previously. This indicates that an energy-transfer process starts to take place. We believe that part of the excitation of isolated Cr^{3+} ions is effectively transferred to pairs of Cr^{3+} ions. Indeed, optical excitation in any of the absorption bands of the isolated Cr^{3+} ions (Fig. 2) do give rise to supplementary emission bands located at 735.2 nm and 734.4 nm (Fig. 7). These two sharp emissions are almost completely polarized. Figure 8 shows a comparison of the excitation spectra of the luminescence emitted by isolated Cr^{3+} pairs at 735 nm. New excitation (and absorption) bands appear especially in the region of the $^4A_2 \rightarrow {}^2E$ and $^4A_2 \rightarrow {}^2T_1$ transitions. However, the bands which belong to isolated Cr^{3+} ions also appear, within the limit of experimental error, at the same positions in the excitation and absorption spectra of the pairs. This also confirms the occurrence of an energy-transfer process between both entities. The decay curve of the pair luminescence is also a pure exponential; its time constant value, $\tau \sim 1$ ms, is almost independent of temperature. An interesting phenomenon has been discovered in the UV region. In crystal II, a series of sharp lines appears in the pair-absorption and excitation spectra at approximately twice the energy of the $^4A_2 \rightarrow {}^2E$ and $^4A_2 \rightarrow {}^2T_1$ transitions (Fig. 9). We believe that these transitions are due to a one-photon double excitation of the Cr^{3+} pairs such as $(^4A_2,{}^4A_2) \rightarrow ({}^2E,{}^2E)$, $(^4A_2,{}^4A_2) \rightarrow ({}^2T_1,{}^2T_1)$ and $(^4A_2,{}^4A_2) \rightarrow ({}^2E,{}^2T_1)$.

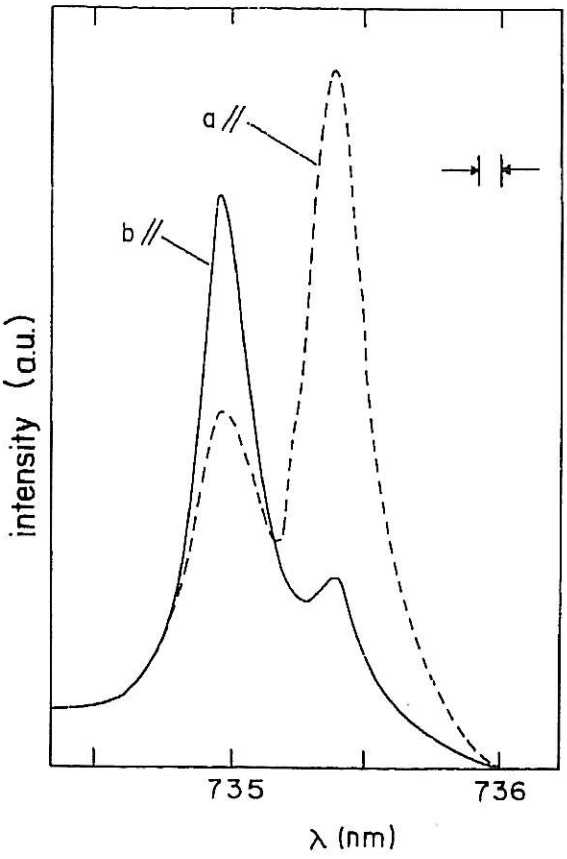

Fig. 7. Emission spectra due to Cr^{3+} pairs measured at T=9 K with light propagating along the c axis and E parallel to the a and b axes. Excitation at 560 nm.

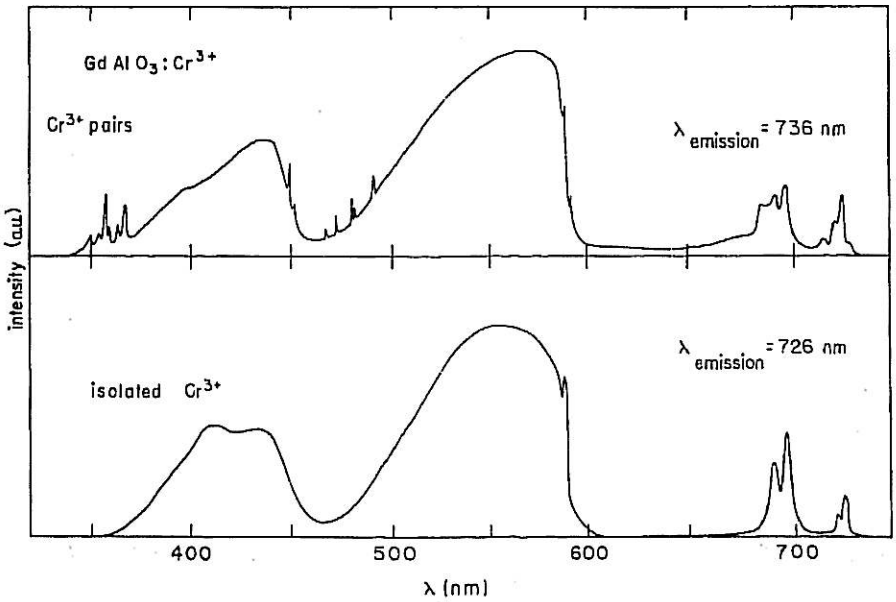

Fig. 8. Excitation spectra of the luminescence emitted by isolated Cr^{3+} ions (726 nm) and Cr^{3+} pairs at 735 nm measured at T=9 K.

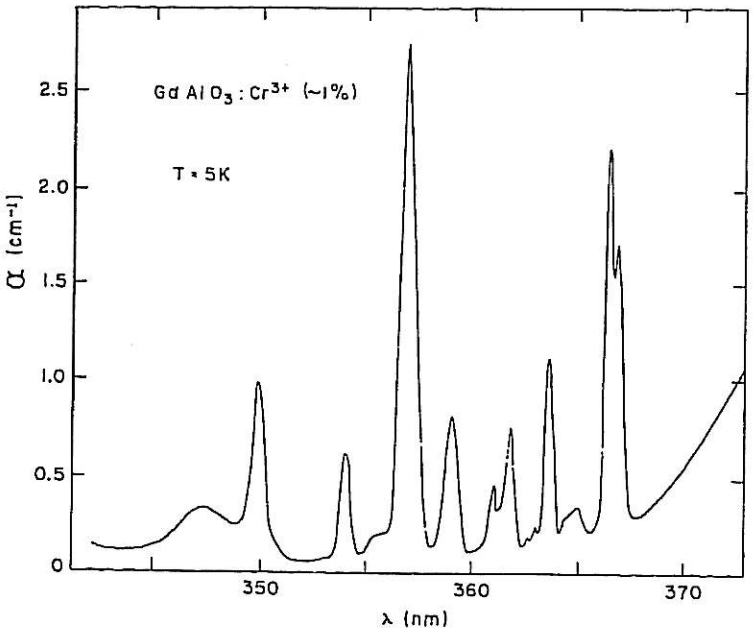

Fig. 9. Absorption spectrum of pairs of Cr^{3+} in the UV region. The transitions belong to one-photon double excitation of the Cr^{3+} pairs.

III Discussion

Although the former theoretical models[12,13,15] based on exchange interactions between Cr^{3+}-Gd^{3+} and Gd^{3+}-Gd^{3+} explain rather well the positions and the number of lines in absorption and emission, as well as some of their behaviors as a function of temperature, they do not allow the explanation of the polarization phenomena and the variation of the transition probability in the antiferromagnetic phase. We recently started calculations based on an extension of the theory of the Zeemann effect developed for ruby by Tanabe and Sugano[21] for which polarization effects have been observed. These results will be presented elsewhere.

Acknowledgements: This work has been supported by CNPq, FAPESP and FINEP (Brazil). We are grateful to Prof. E. Castellano for having oriented a sample and determined its lattice parameters.

References

1. S. Geller, J. Chem. Phys. 24, 1236 (1955)
2. S. Geller and V.B. Bala, Acta Crystallogr. 9, 563 (1956) and 9, 1019 (1956)
3. K.W. Blazey and H. Rohrer, Phys. Rev. 173, 574 (1968)
4. K.W. Blazey, H. Rohrer and R. Webster, Phys. Rev. B4, 2287 (1971)
5. D.C. Cook and J.D. Cashion, J. Phys. C, 9, L97 (1976)
6. A.H. Cooke, N.J. England, N.F. Preston, S.J. Swithenby and M.R. Wells, Solid State Commun. 18, 545 (1976)
7. P.A. Arsenev, H.W. Hassan and M.V. Chukichev, Phys. Stat. Sol. (a) 28 K111 (1975)
8. J.F.B. Hawkes and M.J.M. Leask, J. Phys. C 1, 165 (1968) and 5, 1705 (1972)
9. J. Fengarol and N. Pelletier-Allard, C.R. Acad. Sci. Paris, 272, 901 (1971)
10. C. Coulon and N. Pelletier-Allard, J. Phys. C 7, 454 (1974)
11. K.W. Blazey and G. Burns, Proc. Phys. Soc., London, 91, 640 (1967)
12. J. Murphy and R.C. Ohlmann, Optical properties of ions in crystals, Interscience Publishers, J. Wiley and Sons 1967
13. R.C. Ohlmann, R. Mazelsky and J. Murphy, Technical Report, Westinghouse Laboratories (1967)
14. J.S. Helman, R.A. Carvalho, H. Panepucci, M.C. Terrile, M.A. Aegerter and E. Soares, Solid State Commun. 31, 1015 (1979)
15. J.S. Helman, J. Phys. Chem. Solids 32, 251 (1971)
16. H.J. Scheel and E.O. Schulz-Dubois, J. Cryst. Growth 8, 304 (1971)
17. H.J. Scheel, J. Cryst. Growth 13/14, 560 (1972)
18. J.P. Remeika, J. Amer. Chem. Soc. 78, 4259 (1956)
19. H.J. Scheel and D. Elwell, J. Cryst. Growth 12, 153 (1972)
20. H.C. Basso and M.A. Aegerter, to appear in Appl. Opt., January 1981
21. Y. Tanabe and S. Sugano, J. Phys. Soc. Japan 9, 753 (1954) and 13, 880 (1958)